Improving the Thermal Efficiency of Gasket Plate Heat Exchangers Used in Vegetable Oil Processing

Anișoara Arleziana Neagu and Claudia Irina Koncsag *

Posted Date: 16 December 2024

doi: 10.20944/preprints202412.1271.v1

Keywords: heat transfer; plate heat exchanger; chevron angle; nanofluid; aluminium alloy

 doi:10.20944/preprints202412.1271.v1

Article

Improving the Thermal Efficiency of Gasket Plate Heat Exchangers Used in Vegetable Oil Processing

Anișoara-Arleziana Neagu and Claudia Irina Koncsag *

Chemistry and Chemical Engineering Department, Ovidius University of Constanta, 900527 Constanta, Romania

* Correspondence: ckoncsag@univ-ovidius.ro

Abstract: The study investigates, by calculations, some ways to improve the thermal efficiency of plate heat exchangers used in the vegetable oil processing industry. The performance of these heat exchangers is limited by the heat transfer rate on the oil side and by the low thermal conductivity of the plate material. The study starts from a base case with vegetable oils cooled with water in plate heat exchangers, all with chevron angle 30° and different number of channels and plate transfer area. The change of one geometrical characteristic of the plates, namely the chevron angle, from 30° to 45° then to 60°, led to important increasing of the overall heat transfer coefficients, by 16.0 % when changing from 30° to 45° and by 28.1% on average when increasing the angle from 45° to 60°. This is an important increase accompanied by the rise of the pressure drops in circuits, but the values are acceptable since not exceeding 1 bar on oil circuit and 1.4 bar on cold fluid circuit, respectively. The use of Fe_3O_4–SiO_2/Water hybrid nanofluids with concentration 0.5% v/v, 0,75% v/v and 1% v/v were investigated, to replace the cooling water. An increase by 2.2% on average was noticed when using the 1% v/v nanofluid comparatively with water, which is not large but adds to the chevron angle increasing. A supplementary 2.6% increase is possible by changing the manufacture material for plates with aluminum alloy 6060, also adding to the performances obtained by previous modifications. The total increase for all the set of modification can increase the performance by 34.2% on average. Thus, for the design of new PHEs, the miniaturization of the equipment becomes possible.

Keywords: heat transfer; plate heat exchanger; chevron angle; nanofluid; aluminium alloy

1. Introduction

The plate heat exchangers (PHE) appeared one hundred years ago following the need for compact and more thermally efficient equipment for heat transfer [1]. Now they are widely used in chemical and food industry, among many other industrial applications [2]. The plate heat exchangers developed in a range of construction types: gasket plate-and-frame, brazed, welded, welded plate-and-shell [3]. Gasket plate-and-frame heat exchanger is the oldest type of this category but still popular for its benefits, such as versatility and easy maintenance [1,4], also known for its great thermal efficiency.

Over the years, the geometry of PHEs was improved to enhance the heat transfer. Practicing corrugations with chevron angles in plates was widely adopted to increase the heat transfer area per unit volume [5,6], to create supplementary turbulence or avoiding maldistribution of fluid in the ports [5,6]. Other small improvements were added, with effect on the thermal efficiency and roughness increasing. For example, wire inserts in the channels [7] led to increase of longitudinal turbulence with effect on the performance which enhanced by up to 38% comparing with conventional chevron type plates. Modifying the stainless steel of the plates by electrochemical etching with nitric acid-hydrochloric acid aqueous solution, under a voltage of 5 V, Nguyen et al. [8]

 doi:10.20944/preprints202412.1271.v1

obtained a rougher surface which had as an effect, the increase of heat transfer coefficient by 10.5-17.7%, but also increasing the friction coefficient by 21.3%.

Novel configurations of PHEs appeared, such as new geometry corrugates by repeating a basic half-ellipse cross-section [9] or the pillow-plate channels [10]. They bring some advantages. The repeated half-ellipse cross sections induce transverse disturbances in the fluid, with positive effect on the heat transfer up to 37% over the conventional PHEs [9]. The pillow-plate channel together with an elliptical welding spot in the middle of each unit improve the lateral mixing leading to superior thermal performances, and significantly decrease the pressure loss in the apparatus [10].

For three decades now, the use of nanofluids as cooling agents was extensively studied [11–14], aiming to exploit their superior thermal properties. Nanoparticles enhance the conductivity of conventional fluids. Mononanofluids contain a single type of nanoparticles such as metal, metallic oxides, graphene, etc. For example, carbon nanotubes (CNT) 1% vol enhance the thermal conductivity of ethylene glycol by 12.4% [15] and CeO_2 dispersed at 0.75 % vol in water increased the overall heat coefficient by 28% [16]. Ajeeb et al. [12] reported for nanofluid with 0.2% vol Al_2O_3 in distilled water an increased heat transfer (Nu number) by 27%. Unavoidably, the pressure drops increases too, by 8%.

The hybrid particles synthetized together have a synergistic effect on the thermal conductivity and consequently on the heat transfer rate. For example, the aqueous nanofluid containing 1% vol hybrid particles Fe_3O_4-SiO_2 with 47 nm dimension, increased the number of transfer units (NTU) by 24.51% and the thermal effectiveness by 13.23% [11]. There is a variety of hybrid particles discovered in the latest years (binary oxides, graphene composites with metals or metal-oxides, graphene-polymer composites, etc.) but some were tested on other types of heat exchangers, so need is to focus the thermal efficiency analysis on PHE applications and especially to calculate the overall heat transfer coefficients since they may vary with the geometrical characteristics' dimensions of PHE [14].

To improve thermal-hydraulic performance, new materials for plates were developed: polymer-graphene composite [17], coatings with Ni, Cu, Ag [18], metallic microporous layers [19], some also responding to anticorrosion protection requirements.

The performance of PHEs, was not only tested in the laboratory but also, new equations describing their thermal efficiency were developed and validated [20–22]. These equations are required for sizing the industrial equipment.

Higher efficiency and miniaturization are the new challenges for the heat exchangers development. The overall heat transfer coefficients depend on the convection in fluids on both sides of the separating wall and also on the thermal conductivity of the wall's material. These overall coefficients result lower than the lowest of the partial heat transfer coefficients. Any method to enhance the partial heat transfer coefficients is welcome.

Inspired by the works of forerunners, the present study investigates some solutions for the enhancement of heat transfer in gasket PHEs used in vegetable oil processing industry: modifying the chevron angle of corrugations, the use of Fe_3O_4-SiO2 nanoparticles suspended in the cooling water, and the change of the material for making the plates. The mathematical model of Dović and co-workers [22] validated and published by us previously for the calculation of heat transfer coefficients [23], together with accurate data for thermophysical properties of fluids, were used for the evaluation of the heat exchangers performances.

2. Materials and Methods/Research Method

2.1. Equipment

Three chevron plate heat exchangers, serving as coolers in different stages of vegetable oil processing, were tested with water in a previous work [23]. Their geometrical characteristics are the same (Figure 1), but differences appear in the effective heat transfer number of plates and the size of some elements (corrugation depth b, channel cross sectional flow area A_{ch}) as seen in Table 1, so their total heat transfer areas are different.

 doi:10.20944/preprints202412.1271.v1

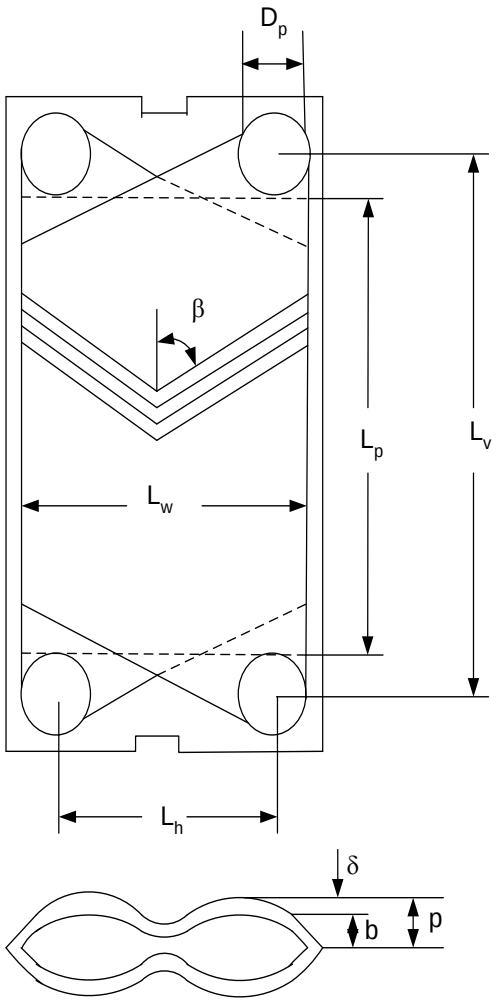

Legend
L_v – Vertical distance between centres of ports;
L_p – Plate length between ports;
L_w – Plate width;
L_h – Horizontal length between centres of ports;
D_p – Port diameter;
d - Plate thickness;
p – Plate pitch;
b – Corrugation depth (amplitude of sinusoidal duct)
b - Corrugation inclination angle relative to vertical direction;

Figure 1. Chevron corrugated plate and its main characteristics.

Table 1. The size of geometrical characteristics of the PHEs.

Geometrical Characteristics of Chevron Plates	**Symbol**	**Heat Exchanger #1**	**Heat Exchanger #2**	**Heat Exchanger #3**
Vertical distance between centres of ports	L_v	1070 (mm	1070 (mm)	1070 (mm)
Plate length between ports (effective length)	L_p (Leff)	858 (mm)	858 (mm)	858 (mm)
Plate width	L_w	450 (mm)	450 (mm)	450 (mm)
Horizontal length between centres of ports	L_h	238 (mm)	238 (mm)	238 (mm)
Port diameter	D_p	212 (mm)	212 (mm)	212 (mm)
Plate thickness	δ	0.6 (mm)	0.6 (mm)	0.6 (mm)
Plate pitch	p	3.17 (mm)	3.14 (mm)	3.14 (mm)
Corrugation depth (amplitude of sinusoidal duct)	b	2.57 (mm)	2.54 (mm)	2.55 (mm)

 doi:10.20944/preprints202412.1271.v1

Corrugation inclination angle relative to vertical direction	β	30°	30°	30°
Hydraulic diameter (=2 b/φ)	d_h	4.396 (mm)	4.34 (mm)	4.5 (mm)
Channel cross-sectional free flow area	A_{ch}	1.116×10^{-3} (m^2)	1.144×10^{-3} (m^2)	1.145×10^{-3} (m^2)
Heat transfer total area	A_e	11.2 (m^2)	9.2 (m^2)	19.7 (m^2)
Total number of plates	N_t	35	28	63
Number of fluid passes	N_p	1	1	1
Number of channels for one pass	N_{cp}	17	13.5	31

2.2. The Research Design

2.2.1. The Base Case

The three PHEs have different technological functions. PHE #1 cools the raw vegetable oil (RO) from 85 °C to 42°C with cooling water (inlet temperature 30°C); PHE #2 cools the bleached oil (BO) from 60 °C to 45°C, and PHE#3 cools the winterized oil (WO) from 110 °C to 40°C. So, there are differences between their thermal load and in the fluids properties which vary with the origin and the temperature. However, the physical properties of raw, bleached and winterized oils are insignificantly different for those of the same vegetal origin.

There were two types of processing oil: sunflower and rapeseed, with density (ρ) and viscosity (μ) variation shown in Figure 2 and Figure 3. These values were determined in laboratory with an apparatus Anton Parr SVM 3000 which measure both density and viscosity on a preset range of temperature.

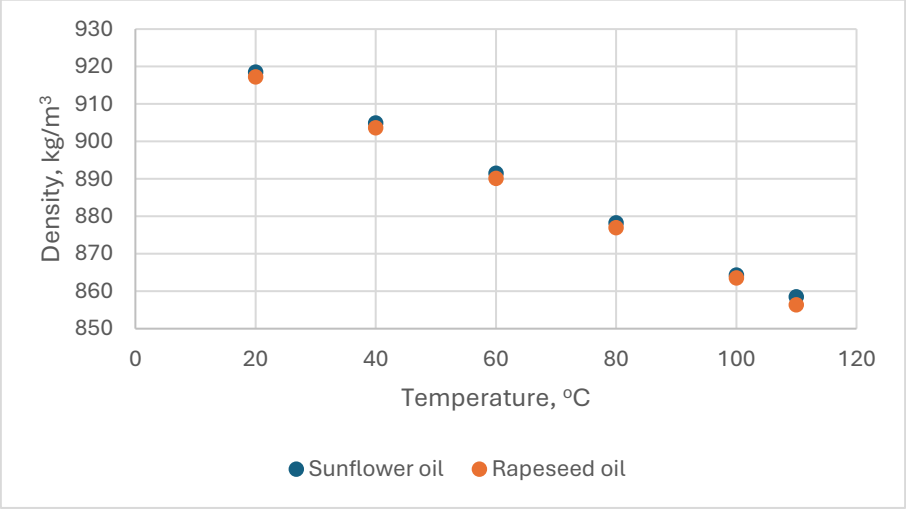

Figure 2. Variation of oils' density with temperature.

Preprints.org (www.preprints.org) | NOT PEER-REVIEWED | Posted: 16 December 2024 doi:10.20944/preprints202412.1271.v1

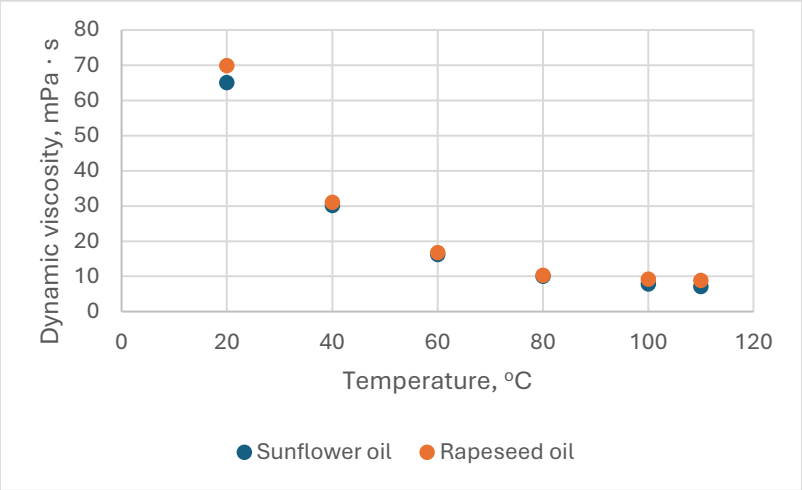

Figure 3. Variation of oils' dynamic viscosity with temperature.

The specific heat capacity (*cp*) and thermal conductivity (λ) values for sunflower oil and rapeseed oil at working temperature were experimentally determined by Hoffmann et al. [24].

The experimental data were collected from three PHEs. In the first part of the experiment, the sunflower oil was processed at four different mass flow rates and in the second part, the rapeseed oil the PHEs ran at one mass flow rate all the campaign long. In total, 15 set of data are available in the base case for the calculations of thermal efficiency and pressure drop.

Table 2. The base case primary data and calculated similarity criteria (Eq. 1-5) for cooling fluid: water and chevron angle β=30°.

Exp.#	PHE #	Oil circuit (hot fluid)				Water circuit (cold fluid)			
		Mass flowrate, kg/s	Re_{sine}	Nu_{sine}	*Pr*	Mass flowrate, kg/s	Re_{sine}	Nu_{sine}	*Pr*
1	1	1.74	17	8.8	211.09	5.25	930	30.7	3.89
2	1	2.05	20	9.5		6.20	1073	34.1	
3	1	2.46	24	10.4		7.43	1297	39.2	
4	1	2.71	26	10.9		8.21	1437	42.2	
5	2	1.94	11	11.6	287.5	2.55	584	21.5	3.89
6	2	2.19	13	12.2		2.88	658	23.4	
7	2	2.49	15	12.9		3.27	748	25.7	
8	2	2.78	15	12.9		3.62	828	27.7	
9	3	1.77	9	5.8	151.0	6.02	600	21.5	3.68
10	3	1.48	10	6.2		7.11	707	24.2	
11	3	1.83	12	6.7		8.52	845	27.5	
12	3	1.95	14	7.0		9.41	936	29.6	
13	1	2.72	18	8.4	202.15	8.23	1443	42.4	3.89
14	2	2.76	17	9.1	267.11	3.62	828	27.6	3.89
15	3	2.72	12	6.0	167.37	9.44	920	29.2	3.68

2.2.2. The Change of Corrugation Angles, Cooling and Material

Previous studies [25,26] have demonstrated that rising the corrugation angles of the plates causes changes in the flow pattern which led to the increase in heat transfer rate. These studies considered the heat exchange between hot water/ cold water (or nanofluid aqueous suspension) and the increase of heat transfer rate was impressive in this case. In our case, the hot fluid is vegetable oil with higher thermal resistance, so the heat transfer rate is expected to be lower. We investigated the

 doi:10.20944/preprints202412.1271.v1

rise of the corrugation/chevron angle from 30° to 45° and 60°, respectively, by observing the influence of the angle on the heat transfer coefficients and on the pressure drop in the heat exchangers.

The overall heat transfer coefficients in the studied heat exchangers are low due to the vegetable oil fluid partial coefficient, so a solution for increasing the heat transfer rate on the water side is to search for another fluid to replace the water. From the multitude of nanofluids experimented in literature, the majority are designed for refrigeration circuits; we chose an aqueous suspension of nanofluid, with better physical properties when working at fluid temperatures between 30-40 °C, the Fe_3O_4–SiO_2/Water hybrid nanofluids. Since some of properties of nanofluids are frequently calculated using the laws for common mixtures [27,28], which can introduce big errors in case of hybrid materials suspensions, it is preferable to have all the physical propertied experimentally determined. In the article [29], density, viscosity, specific heat coefficient, thermal conductivity of Fe_3O_4–SiO_2/Water hybrid nanofluids, varying with temperature, for solid content in suspension in range 0-1% volume concentration were determined experimentally. Then the partial heat transfer coefficients in the hot loop of the heat exchangers and the overall ones were compared between water and nanofluids with 0.5%, 0.75% and 1% vol. Fe_3O_4–SiO_2. Also, the influence on the pressure drop in the apparatus was quantified as a function of the solid concentration in nanofluid.

Usually, the plates of PHEs are manufactured from stainless steel, a cheap and corrosion/erosion resistant material but with small thermal conductivity (cca.15 W/m K) compared with plain carbon steel (cca. 70 W/m K) at the working temperatures of the heat exchangers. It is desirable to find an affordable material with consistently higher conductivity to influence positively the heat transfer. The aluminum alloy 6060, with λ= 207 W/mK, possesses other attractive qualities: good processability and good weldability, making it prone for complex cross sections manufacture. The calculation of overall heat transfer coefficients was made for this material at the optimum case (corrugation angle, nanofluid) considered so far, and the coefficients were compared with those in case of stainless steel.

3. Model

An approach frequently found in literature for heat transfer efficiency [25,27], is to plot Nu vs. Re, where Nu and Re are Nusselt and Reynolds, respectively. According to Dović and co-authors' model (Eq. 8), Nu and Re are redefined taking into consideration the cell's sine duct as Nu_{sine} and Re_{sine} [22]. This model was validated in a previous work [23] and proved to be reliable.

Nu_{sine} numbers serve to calculate the partial heat transfer coefficients on each fluid side (Eq.1):

$$Nu_{sine} = 0.38 \cdot 0.40377 \cdot (4 \cdot f_{app} Re_{sine}^2 \cdot \frac{d_{h,sine}}{L_{furr}})^{0.375} Pr^{1/3} \left(\frac{\mu}{\mu_w}\right)^{0.14} \quad (1)$$

where $L\,furr$=b/sin(2β) is the furrow characteristic length, $d_{h,sine}$ is the hydraulic diameter of the sine duct, and f_{app} is the apparent friction factor which takes into account the flow through sine duct. f_{app} is calculated with Eq. 2:

$$f_{app} = \frac{C}{Re_{sine}} + B \quad (2)$$

B and C are constants depending on the channel geometry.

Eq. 3 and Eq. 4 serve the calculation of Re_{sine} number:

$$Re_{sine} = \frac{u_{sine} d_{h,sine}}{\nu} \quad (3)$$

$$u_{sine} = \frac{\dot{m}_{ch}}{\rho \cdot A_{ch,sine}} \quad (4)$$

where u_{sine} is the the average velocity in the cell's sine duct in furrow direction [m/s], υ is the kinematic viscosity [m²/s], $\dot{m}_{ch}$ is the mass flowrate in the channel [kg/s] and $A_{ch,sine}$ is the channel cross-section transverse to the furrow [m²].

After calculating Nu_{sine} for the cell sine duct, Nu number for the whole cell is calculated with Eq.5:

$$Nu = \frac{Nu_{sine} \times dh}{dh_{sine}} \quad (5)$$

Hence, the partial heat transfer coefficients on hot circuit (h_h) and on cold circuit (h_c) respectively, are:

$$h_h = \frac{Nu_h \times \lambda_h}{dh} \; ; \; h_c = \frac{Nu_c \times \lambda_{hc}}{dh} \quad (6)$$

A more detailed presentation of this model is made in work [23].

Preprints.org (www.preprints.org) | NOT PEER-REVIEWED | Posted: 16 December 2024 doi:10.20944/preprints202412.1271.v1

Then the overall coefficient U is calculated with Eq.7:

$$U = \frac{1}{h_h} + \frac{\delta}{\lambda_{plate}} + \frac{1}{h_c} \quad (7)$$

where δ- plate thickness [m], and λ- metal thermal conductivity [W/m s].

For the calculation of the total pressure drop, one has to take into consideration the pressure drop in cells (Δp_c) and the pressure drop in the ports (Δp_r), summed up to give the total pressure drop (Δp). Since the cells work in parallel, the pressure drop in the cells equals the pressure drop in one cell. The equations 8-14 are used to calculate the pressure drop on both fluids sides.

$$\Delta p = \Delta p_c + \Delta p_r \quad (8)$$

$$\Delta p_c = 4 \times f \times \frac{L_{ef} \times N_p}{dh} \times \frac{G_{ch}^2}{2\rho} \times \left(\frac{\mu}{\mu_w}\right)^{-0.17} \quad (9)$$

where G_{ch} is the mass flow in the channel (kg m^{-2}s^{-1}), μ - the fluid dynamic viscosity at the average temperature in the apparatus, μ_w – the viscosity at the wall, and L_{ef}, N_p , dh are geometrical characteristics (Table 1).

$$\Delta p_r = 1.4 \times N_p \times G_p^2/2\rho \quad (10)$$

where G_p is the mass flow in the ports (kg m^{-2}s^{-1}); Δp_r is negligible (units or dozens N/m^2) in relation to Δp_c, (bar), however it is common to take into consideration this term for the accuracy of the calculation.

The friction factor f is correlated with then the apparent friction factor f_{app} (Eq.2), by Eq.11.

$$f = \frac{f_{app} \times dh}{2(\cos\beta)^3 \times dh_{sine}} \quad (11)$$

3. Results and Discussion

3.1. Changing the Chevron Angle of Plates

The Nu_{sine} and Re_{sine} were calculated with Eq.1, respectively with Eq.3 on both fluid sides, for water as cooling fluid, at β=30°, then 45° and 60°. There were compared the results for the three chevron angles in a graph Nu_{sine} vs. Re_{sine} (Figure 4). Then, the partial heat transfer coefficients, h, were calculated with Eq.4-6 and plotted versus Re_{sine} (Figure 5).

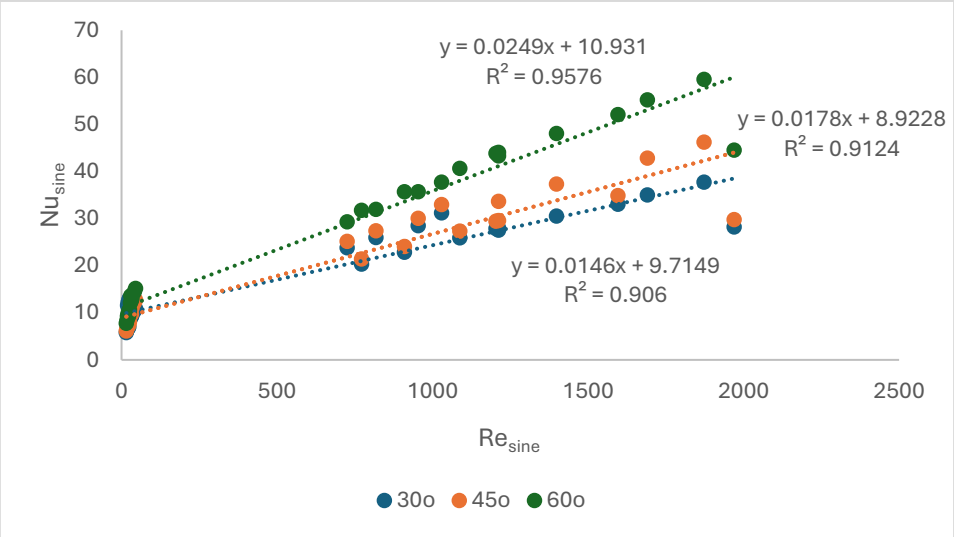

Figure 4. Nu_{sine} vs. Re_{sine} in the fluid circuits of PHEs with corrugation inclination angle relative to vertical direction β= 30°, 45° and 60°.

Preprints.org (www.preprints.org) | NOT PEER-REVIEWED | Posted: 16 December 2024 doi:10.20944/preprints202412.1271.v1

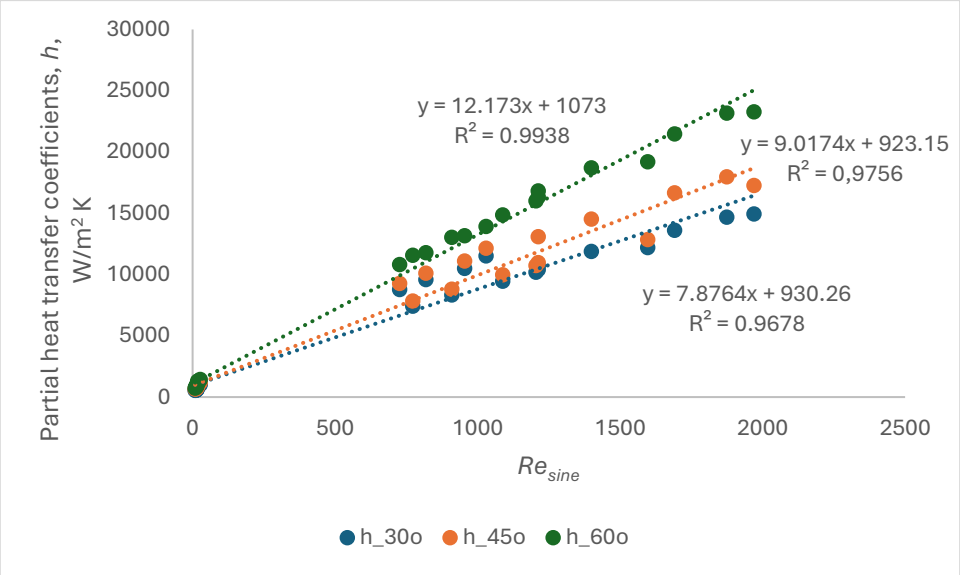

Figure 5. Partial heat transfer coefficients in PHEs with corrugation inclination angle relative to vertical direction β= 30°, 45° and 60°.

Both plots indicate that the heat transfer rate increases with Re_{sin} confirming that turbulence favors the heat transfer. The variation is linear, with correlation coefficients $r^2 > 0.9$. It is interesting that all values for a certain chevron angle are stringed on the same line whatever is the fluid, oil or water, knowing that they are fluids with very different physical properties. This could be explained by the influence of the plate geometry favoring the good mixing and uniformity of flow and temperature in the channel section.

The increasing of the heat transfer rate with chevron angle is important, by 14.8% average when passing from 30° to 45°, and 28.1% average when passing from 45° to 60°. This is an indication that building plates with larger chevron angle in the range 30°-60° may improve substantially the performance of the heat exchanger. Sadeghianjahromi and co-authors [25] demonstrated this by experiment, in the range 35°-50°- 65°, with the mention that the increase from 50 to 65° is much larger than the difference between 35°-50°, tendency confirmed by our data.

The overall heat transfer coefficients *U* were calculated with Eq.7 and the results are presented in Table 3.

Table 3. The increase of overall heat transfer coefficients *U* with increasing the chevron angle *.

Data set #	$U_{30°}$	$U_{45°}$	$U_{60°}$	(%) 30-45	(%) 45-60
1	544	747	828	37.3	52.1
2	606	807	894	33.1	47.4
3	681	881	979	29.2	43.6
4	729	922	1027	26.4	40.9
5	525	609	615	16,1	17.1
6	622	643	669	3.5	7.6
7	613	681	691	11.1	12.7
8	645	686	729	6.4	13.0
9	409	492	505	20.3	23.4
10	447	529	542	18.3	21.3
11	502	571	588	13.8	17.0
12	533	587	614	10.2	15.2
13	767	787	1059	2.7	3.0

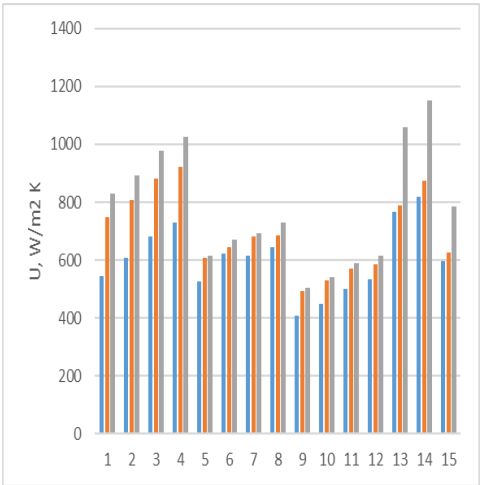

 doi:10.20944/preprints202412.1271.v1

14	820	872	1152	6.4	40.4
15	598	626	786	4.7	3.5
Average increase, %				16.0	28.1

*Legend: ■ chevron angle 30° ■ chevron angle 45° ■ chevron angle 60° .

The overall heat transfer coefficients are smaller than the partial coefficients in Eq.7, namely smaller than the smallest value between h_c, and h_r. Also, the differences when passing from angle 30° to 60° is smaller than that for the partial coefficients. However, an important increase of the overall heat transfer coefficients is noticed which can count for a better thermal performance of the apparatus.

The influence of the chevron angle on the pressure drop in the apparatus can be evaluated, at a first glance, by comparing the friction factors at 30°, 45° and 60°, both on water and oil circuits (Figure 6 a, b). The plot f vs. Re_{sin} shows that values of f on oil circuit are larger than those for water circuit. It is explained by Re_{sin} which is smaller for the laminar flow as it comes across the oil flow. According to Eq. 2 corroborated with Eq.11, the smaller Re_{sine} is, the bigger f_{app} is and, by consequence the the bigger f is. Both family curves respect the exponential trend with correlation coefficients 0.93-0.95 for oil and >0.90 for water. The friction coefficients for water are in the asymptotic zone of the exponential curve, this is why their variation appears linear. In Figure 6 a and b, it is obvious that increasing the chevron angle will lead to the rise of f values.

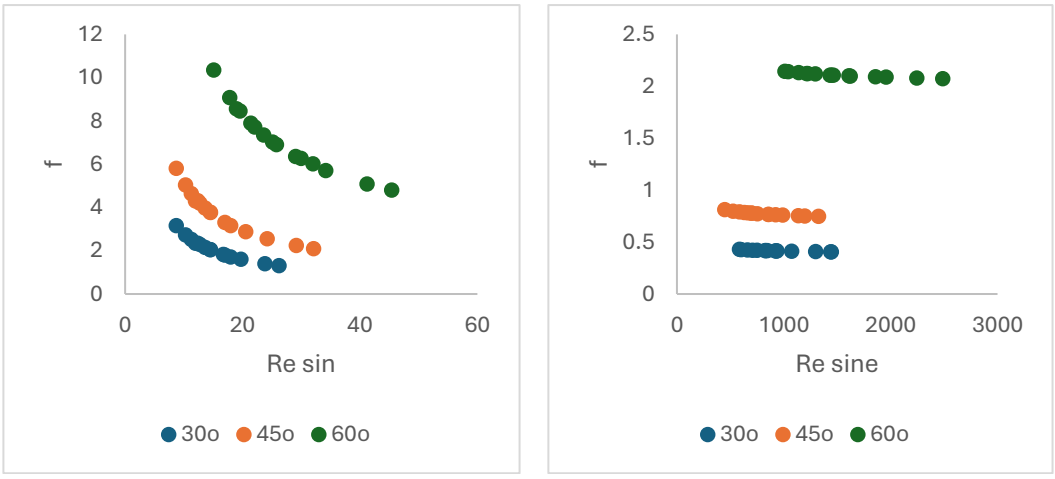

(**a**) (**b**)

Figure 6. The variation of friction factor in the oil circuit (a) and in the water circuit (b) of the PHEs.

The calculated pressure drops also indicate the increase of the values with the corrugation angle, both on water and oil circuits, as seen in Figure 7 a and b. The pressure drops are larger on the water circuit than on the oil's, even though the friction factors are smaller in water channels. This is due to the mass flow square G_{ch}^2 much larger for the water circuit (see Eq.9).

Preprints.org (www.preprints.org) | NOT PEER-REVIEWED | Posted: 16 December 2024 doi:10.20944/preprints202412.1271.v1

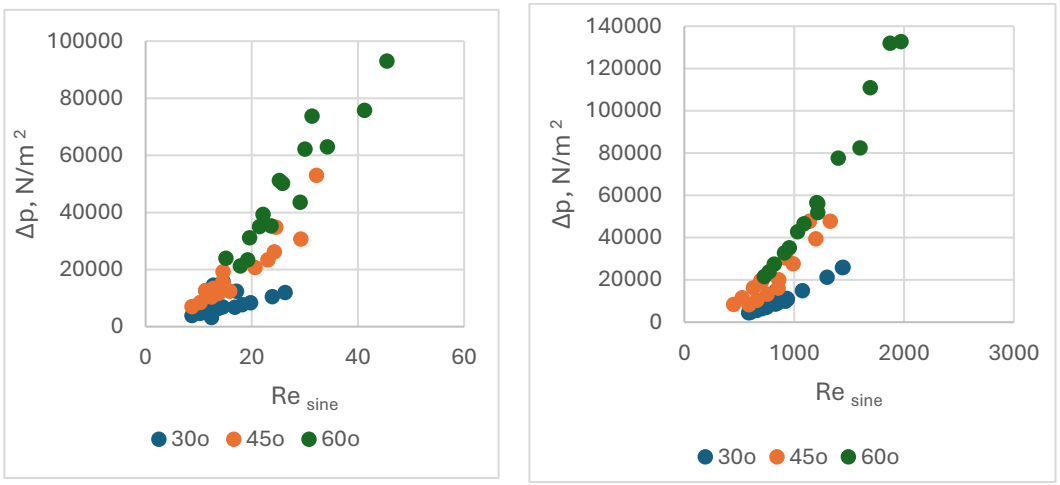

(**a**) (**b**)

Figure 7. The variation of pressure drops in the oil circuit (a) and in the water circuit (b) of the PHEs.

For an apparatus keeping all geometrical characteristics except the corrugation angle, in the oil circuits, the pressure drops Δp increase by 133,2% on average when changing the angle from 30° to 45°, and by 462.6% from 30° to 60°. The figures are comparable for the water circuit, Δp increasing by 86.4% from 30° to 45°, and 414.3% from 30° to 60°, respectively. It is important to note that the pressure drop values are acceptable even for corrugation angle 60°, where the maximum values are below 1.0 bar for oil and below 1.4 bar for water. These data corroborated with the important gains in heat transfer rate when changing the chevron angle from 30° to 60°, suggest that this solution should be taken into consideration further.

3.2. Changing Water with Nanofluids as Cooling Medium

A nanofluid with good physical properties able to increase *Pr* numbers ($=\frac{c_p \mu}{\lambda}$), should be preferred to improve the performance of PHEs. The Fe_3O_4–SiO_2/Water hybrid nanofluids were selected from other aqueous suspensions since they have very good thermal conductivity, higher viscosity than water at working temperatures, even if the specific heat coefficient c_p is slightly poorer. *Pr* numbers increased with concentration of solid in suspension, in our case, up to 16.9% for the suspension with 1% Fe_3O_4–SiO_2. The concentration of these nanofluids is limited to 1% [29] due to the sharp increase of the viscosity over this concentration which can produce disturbances in the flow through the apparatus.

The partial heat transfer coefficients for the cold fluid h_c were calculated, also were the overall coefficients for the PHEs with chevron angles 30°, 45°, 60° and fluids with 0.5%, 0.75% and 1% Fe_3O_4–SiO_2 nanofluids (nf), then compared with water as cooling fluid. The results are summarized in Tables 4–6, for all 15 sets of data in the base case.

Table 4. Partial h_c and overall heat transfer coefficients *U* for chevon angle 30° on water circuit comparatively with nanofluids [W/m²K].

Data set #	h_c water	h_c 0.5%nf.	h_c 0.75% nf.	h_c 1% nf.	U water	U 0.5% nf.	U 0.75% nf.	U 1% nf.
1	10358	11010	11451	11425	544	545	547	549
2	11550	12391	12498	12665	606	608	609	613
3	13538	14100	14005	14525	681	682	683	684
4	14420	15171	15396	15650	729	731	733	755
5	7424	7768	7877	7973	525	530	533	555
6	8099	8461	8516	8690	622	623	625	630

 doi:10.20944/preprints202412.1271.v1

7	8858	9275	9399	9506	613	630	632	644
8	9546	9985	10007	10216	645	646	646	649
9	7058	7457	7536	7609	409	411	414	417
10	7676	8470	8180	8379	447	448	449	451
11	8439	8756	8814	9517	502	503	504	507
12	9243	9788	9926	10128	533	534	536	539
13	10181	10281	10399	10860	767	781	783	785
14	10495	10646	10788	11211	820	828	841	855
15	10925	11032	11261	11832	598	612	616	615

Table 5. Partial h_c and overall heat transfer coefficients U for chevon angle 45° on water circuit comparatively with nanofluids [W/m²K].

Data set #	h_c water	h_c 0.5%nf.	h_c 0.75% nf.	h_c 1% nf.	U water	U 0.5% nf.	U 0.75% nf.	U 1% nf.
1	10850	12207	12432	13190	747	753	754	767
2	12038	13772	14023	14875	807	815	816	826
3	13821	15725	16009	16979	881	890	891	902
4	14899	16910	17214	18254	992	1003	1005	1018
5	8101	8577	8827	9264	609	616	616	624
6	8835	9361	9632	10106	643	650	651	660
7	9694	10254	10549	11066	681	689	690	698
8	10624	11030	11346	11899	686	695	695	702
9	7245	8979	9059	9570	492	497	497	502
10	8135	10110	10197	10769	529	535	536	542
11	9241	11523	11619	12267	571	577	577	586
12	9945	12379	12481	13175	587	594	595	601
13	11240	11951	12944	13617	787	795	796	802
14	11042	12240	12350	12621	872	877	879	887
15	9722	9864	9993	12798	626	631	631	637

Table 6. Partial h_c and overall heat transfer coefficients U for chevon angle 60° on water circuit comparatively with nanofluids [W/m²K].

Data set #	h_c water	h_c 0.5%nf.	h_c 0.75% nf.	h_c 1% nf.	U water	U 0.5% nf.	U 0.75% nf.	U 1% nf.
1	12085	16249	17077	17493	828	839	840	843
2	13629	18322	18975	19757	894	904	906	908
3	15558	20946	21823	22583	979	993	994	996
4	16728	22557	23546	24297	1027	1036	1038	1041
5	8361	11230	11718	12231	616	627	628	630
6	9122	12271	12786	13346	669	681	682	684
7	9990	13458	14039	14638	691	702	704	706
8	10743	14488	15131	15758	729	742	743	745
9	8843	11793	12579	13066	505	508	510	511
10	9952	13299	14186	14727	542	547	548	549
11	11338	15180	16194	16786	588	593	594	596
12	12178	16320	17411	18098	614	628	629	631
13	14785	16918	22601	23249	1059	1073	1075	1077
14	12773	15932	18571	19285	1152	1172	1176	1220

 doi:10.20944/preprints202412.1271.v1

15	12124	15248	16358	16658	786	796	798	800

The results in Tables 4-6 show an important increase of partial heat transfer coefficients in the cooling circuit with the concentration of Fe_3O_4–SiO_2 in the nanofluid: with up to 8.4% for the angle 30°, 22.8% for 45°, and 46,9% for 60°. However, the effect on the overall transfer coefficient is much smaller but not negligible: 2.2% for 30°, 2.3% for 45° and 2.1% for 60°, when increasing the concentration of Fe_3O_4–SiO_2 from 0 to 1%. This adds to the increase of the overall coefficients obtained when increasing the chevron angle.

The effect of changing the water with Fe_3O_4–SiO_2/Water hybrid nanofluids on the pressure drop is illustrated in Figure 8 a, b, c. As seen, the pressure drop in a PHE increases moderately with the concentration of Fe_3O_4–SiO_2. By increasing the concentration from 0% to 1%, the pressure drops increases with 6.6% for the PHEs having chevron angles 30°, 4.7% for angle 45° and with 5.8% for 60°. The rise of the pressure drop because of the used nanofluid is much lower when compared with the increase because of changing the chevron angle and adds to that, without affecting it decisively.

3.3. Changing the Plate Material

When choosing the aluminum alloy 6060 for further calculations, the main reason was its very good thermal conductivity λ= 207 W/m K compared with the stainless steel (λ= 15 W/m K), the material from which are made the plates of PHEs. In addition, it is appropriate for the manufacture of the plates considering its good processability.

In previous calculations, the best overall heat transfer coefficients were obtained for plates with corrugation angle 60° and replacing the water as cooling fluid with 1% v/v Fe_3O4–SiO_2 nanofluid. The pressure drops in PHEs in the new conditions were acceptable, with values under 1.5 bar. So, the overall heat transfer coefficients were recalculated with Eq. 7, were only the λ_{plate} was replaced. The results are presented in Table 5a.

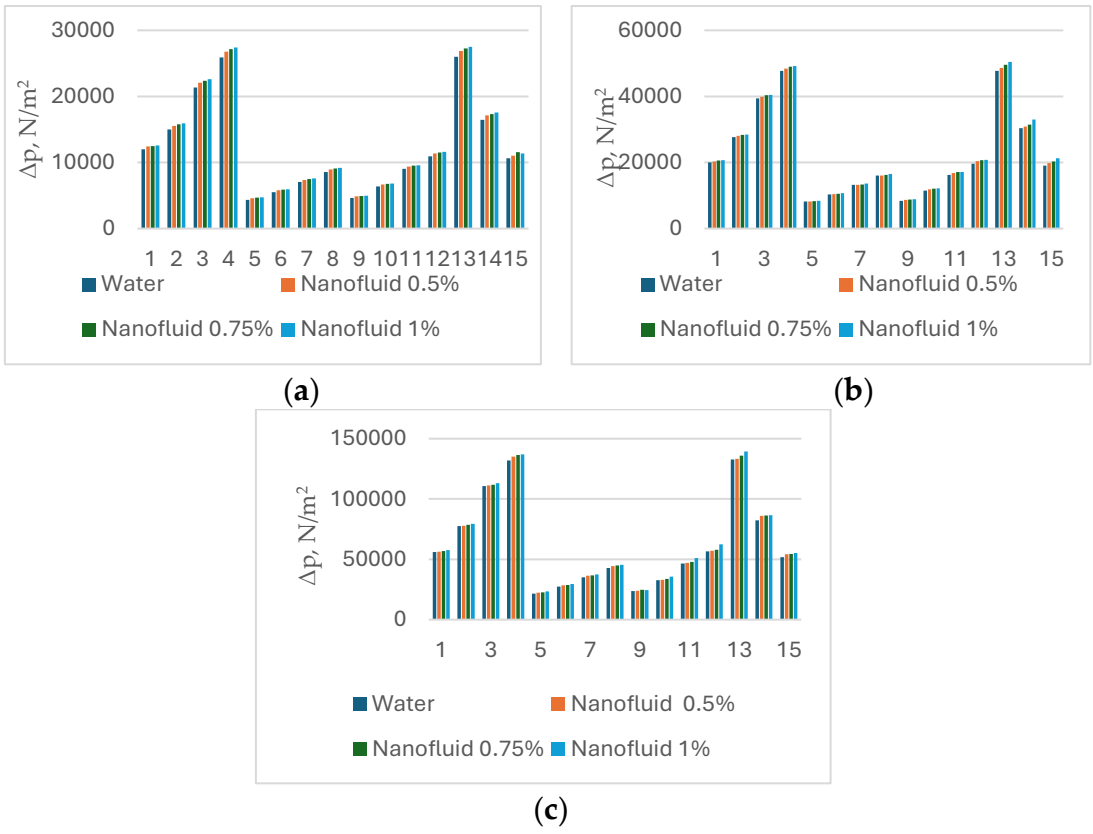

Figure 8. The variation of pressure drops in the on the water circuit comparatively with nanofluids for PHEs with chevron angles 30° (a), 45° and 60°.

 doi:10.20944/preprints202412.1271.v1

Table 5. The overall heat transfer coefficients for β=60° nanofluid 1%v/v and plate manufactured from alloy 6060 compared with the base case.

Data set #	U [W/m K] β=30° fluid: water stainless steel plate Base case	U [W/m K] β=60° nanofluid 1%, stainless steel plate	U [W/m K] β=60° nanofluid 1% Alloy 6060 plate Final choice	U increasing for changing the material β=60° nanofluid 1%	U increasing from the base case to final choice %
1	544	843	860	2.0	58.1
2	606	908	929	2.3	53.2
3	681	996	1022	2.6	50.0
4	729	1041	1070	2.7	46.7
5	525	630	644	2.3	22.7
6	622	684	701	2.5	12.7
7	613	706	724	2.6	18.1
8	645	745	765	2.7	18.7
9	409	511	519	1.5	26.8
10	447	549	558	1.7	24.9
11	502	596	607	1.9	20.9
12	533	631	644	2.0	20.7
13	767	1077	1121	4.1	46.1
14	820	1220	1275	4.5	55.5
15	598	800	824	3.0	37.7
Average increase:				2.6%	34.2%

The average increase of U only by changing the material is 2.6%. As calculations went, by adopting the chevron angle β=60°, the hybrid nanofluid Al_2O_3-SiO_2 with 1% v/v concentration and the aluminum alloy 6060 as manufacture material, the overall heat transfer coefficients increase by 12.7-58.1% for each PHE, with an average of 34.2%. This is an important increasing, considering the resistance that the vegetable oil imposes to the heat transfer rate.

4. Conclusion

Looking for solutions with the aim to improve the heat transfer in PHEs used in the vegetable oil processing industry, the following ways were searched: changing the corrugation inclination angle relative to vertical direction, replacing the water as cooling medium with appropriate nanofluid and replacing the material for plate manufacture with an alloy with better thermal conductivity.

The findings of our study are the following:

The biggest influence on the PHEs performances was when increasing the corrugation angle from β=30° to β=45°, then to β=60°. Since the rise of partial heat transfer coefficients h_c was spectacular, the overall coefficients (U) increased less but this was an important rise, by 16.0 % when changing from 30° to 45° and by 28.1% from 45° to 60°. When increasing the corrugation angle from β=30° to β=60°, the pressure drops increase by 462.6% on average in the oil circuit and by 414.3% on average in the cooling fluid circuit. The values of pressure drops are acceptable on both fluids sides since not exceeding 1 bar in oil and 1.4 bar in cold fluid circuit, respectively.

The use of Al_2O_3-SiO_2/Water hybrid nanofluid as cooling medium also improves the thermal efficiency of the PHEs by 2.2% on average, also increasing with the concentration of solid in fluid, but this is limited to 1% v/v because of the sharp increase of the fluid viscosity over this concentration.

Changing the manufacture material for plates with aluminum alloy improves the heat transfer coefficients by 2.6 % on average and the total increase for all the set of modification can increase the performance by 34.2% on average. For the design of new PHEs, the miniaturization of the equipment becomes possible.

Author Contributions: Conceptualization, methodology, software, validation, investigation, A.-A.N. and C.I.K.; project administration, data curation and writing-original draft preparation, A.-A.N.; supervision, writing-review and editing, C.I.K. All authors have read and agreed to the published version of the manuscript.

Funding: This research received no external funding

Data Availability Statement: Primary data were obtained from our original experiment. All processed data are included in this article and are available for further processing and interpretation by other authors.

Conflicts of Interest: The authors declare no conflicts of interest.

References

1. Yang, J., Jacobi, A., Liu, W. Heat transfer correlations for single-phase flow in plate heat exchangers based on experimental data, *App.Therm. Eng.* **2017**, *113*, 1547-1557.
2. Hedayati, S., Ansarifar, E., Jafari, M.S. Thermal processing of food products by steam and hot water, Elsevier: Cambridge, UK, 2023, p.111-128.
3. Arsenyeva, O.; Tovazhnyanskyy, L.; Kapustenko, P.; Klemeš, J.J.; Varbanov, P.S. Review of Developments in Plate Heat Exchanger Heat Transfer Enhancement for Single-Phase Applications in Process Industries. *Energies* **2023**, *16*, 4976.
4. Kumar, S., Kumar Singh, S., Sharma, D. Comprehensive Review on Thermal Performance Enhancement of Plate Heat Exchanger, *Int.J.Thermophys.* **2022**, *43*:109.
5. Sri Valli, G., Kommineni, R., Sreedhara Rao, B. A Literature Review on Corrugated Plate Heat Exchanger, *Mater. Today*. **2019**, *18*, 320-326.
6. Elmaaty, T.M.A.; Kabeel, A.E.; Mahgoub, M. Corrugated plate heat exchanger review. *Renew. Sust. Energ. Rev.* **2017**, *70*, 852–860.
7. Nitesh K. Panday, Shailendra N. Singh. Study of thermo-hydraulic performance of chevron type plate heat exchanger with wire inserts in the channel, *Int. J. Therm. Sci*. **2021**, *173*, 107360.
8. Nguyen, D.H., Kim, K.M., Shim, G.H., Kim, J.H., Lee,Ch.H., Lim, S.T., Ahn, S.H. Experimental study on the thermal-hydraulic performance of modified chevron plate heat exchanger by electrochemical etching method, *Int. J. Heat Mass Transf.* **2020,** *155*, 119857.
9. Khail, A.A., Erişen, A. Heat transfer and performance enhancement investigation of novel plate heat exchanger, *TSEP* **2022**, *34*, 101368.
10. Piper, M., Zibart, A., Kenig, E.Y. Design equations for turbulent forced convection heat transfer and pressure loss in pillow-plate channels, *Int. J. Therm. Sci*. **2017**, *120*, 459-468.
11. Syam Sundar, L., Chandra Mouli, K.V.V. Effectiveness and number of transfer units of plate heat exchanger with Fe3O4–SiO2/Water hybrid nanofluids: Experimental and artificial neural network predictions, *Case Stud. Therm. Eng*. **2024**, *53*, 103949.
12. Ajeeb, W., Thieleke da Silva, R.R.S, Sohel Murshed, S.M. Experimental investigation of heat transfer performance of Al2O3 nanofluids in a compact plate heat exchanger, *Appl.Therm. Eng.* **2023**, *218*, 119321.
13. Chen, T., Kim, J., Cho, H. Theoretical analysis of the thermal performance of a plate heat exchanger at various chevron angles using lithium bromide solution with nanofluid, *IJR* **2014**, *48*, 233-244.
14. Syam Sundar, L. Synthesis and characterization of hybrid nanofluids and their usage in different heat exchangers for improved heat transfer rates: A critical review, *JESTEC* **2023**, 44, 101468.
15. Liu, M.-S., Lin, M.-C.-C., Huang, I.-T., Wang, C.-C. Enhancement of thermal conductivity with carbon nanotube for nanofluids, *Int. Comm. Heat Mass Transf.* **2005**, *32*, 1202-1210.
16. Tiwari, A.K., Ghosh, P., Sarkar, J. Heat transfer and pressure drop characteristics of CeO2/water nanofluid in plate heat exchanger, *Appl. Therm. Eng.* **2013**, *57*, 24–32.
17. Kiepfer, H., Stannek, P., Grundler, M., Bart, H-J. Development and thermal performance of a thermoplastic-graphite-composite based plate heat exchanger for use in corrosive media, *App. Therm. Eng*. **2024**, *236*, 121581.
18. Nguyen, D.H., Kim, K.M., Nguyen Vo, T.T., Shim, G.H., Kim, J.H., Ahn, H.S. Improvement of thermal-hydraulic performance of plate heat exchanger by electroless nickel, copper and silver plating, *Case Stud. Therm. Eng*. **2021**, *23*, 100797.
19. Wajs, J., Mikielewicz, D. Influence of metallic porous microlayer on pressure drop and heat transfer of stainless steel plate heat exchanger, *Appl. Therm. Eng*. **2016**, 93, 1337-1346.
20. Arsenyeva, O.; Tovazhnyansky, L.; Kapustenko, P.; Khavin, G. Mathematical Modelling and Optimal Design of Plate-and-Frame Heat Exchangers. *Chem. Eng. Trans*. **2009**, *18*, 791–796.
21. Martin, H. A theoretical approach to predict the performance of chevron-type plate heat exchangers. *Chem. Eng. Process Process. Intensif.* **1996**, *35*, 301–310.
22. Dović, D.; Palm, B.; Švaić, S. Generalized correlations for predicting heat transfer and pressure drop in plate heat exchanger channels of arbitrary geometry. *Int. J. Heat Mass Transf.* **2009**, *52*, 4553–4563.

 doi:10.20944/preprints202412.1271.v1

23. Neagu A.A., Koncsag, C.I. Model Validation for the Heat Transfer in Gasket Plate Heat Exchangers Working with Vegetable Oils. *Processe*s. **2022**, *10*, 102.
24. Hoffmann, J.-F., Vaitilingom, G., Henry, J.-F., Chirtoc, M., Olives, R., Goetz, V., Py, X. Temperature dependence of thermophysical and rheological properties of seven vegetable oils in view of their use as heat transfer fluids in concentrated solar plants, *Sol. Energy Mater. Sol. Cells*. **2018**, *178*, 129-138.
25. Sadeghianjahromi, A., Jafari, A., Wang, Chi-Chuan. Numerical investigation of the effect of chevron angle on thermofluids characteristics of non-mixed and mixed brazed plate heat exchangers with experimental validation, *Int. J. Heat Mass Transf.* **2022**, *184*, 122278.
26. Kumar Tiwari, A., Said, Z., Pandya, N.S. , Shah, H. Effect of plate spacing and inclination angle over the thermal performance of plate heat exchanger working with novel stabilized polar solvent-based silicon carbide nanofluid, *J. Energy Storage*. **2023**, *60*, 106615.
27. Khan, A.A., Danish, M., Rubaiee, S. Yahya, S.M. Insight into the investigation of Fe3O4/SiO2 nanoparticles suspended aqueous nanofluids in hybrid photovoltaic/thermal system, *CLCE*, **2022**, *11*, 100572.
28. Syam Sundar, L., Chandra Moulib, K.V.V., Effectiveness and number of transfer units of plate heat exchanger
29. with Fe3O4–SiO2/Water hybrid nanofluids: Experimental and artificial neural network predictions, *Case Studies Therm. Eng*. **2024**, *53*, 103949.
30. Alklaibi, A.M., Chandra Mouli, K.V.V., Syam Sundar, L. Heat transfer, and friction factor of Fe3O4–SiO2/Water hybrid nanofluids in a plate heat exchanger: Experimental and ANN predictions, *Int.J.Therm.Sci*. **2024**, *195*, 108608.